Measuring Spin Precession in the Ringdown

Interim Report I, LIGO Student Undergraduate Research Fellowship, California Institute of Technology

Serena Fink
University of Montana, Missoula, MT 59801

Mentors: Simona Miller and Dr. Eliot Finch
LIGO Laboratory, Caltech, Pasadena, CA 91125

(Dated: July 9, 2025)

The effect of the progenitor masses and spins on the inspiral phase of a gravitational-wave signal from a binary black hole (BBH) merger is relatively well understood for the case where spins are aligned with the orbital angular momentum. However, less is known about how progenitor properties, especially misaligned spins, impact the ringdown portion of the signal. Therefore, it is an open question what we can infer about inspiral parameters from the ringdown alone. As several of the high-mass (most ringdown-dominated) BBH systems observed by LIGO have misaligned spins, the ability to predict inspiral properties from the ringdown would give us great insight into this portion of the BBH population. This project aims to extract quasinormal modes from the ringdown signal in simulated gravitational-wave signals to determine if and how well those modes can accurately infer information about the inspiral. If what these modes predict is consistent with the properties of the simulation, this could be applied to real gravitational wave data to infer inspiral parameters.

I. INTRODUCTION

A binary black hole (BBH) coalescence can be broken into three parts: the inspiral, the merger, and the ringdown. The inspiral period describes when the two BHs are orbiting each other and emitting lower frequency gravitational waves (GWs) as they get closer together, and then eventually collide in the merger. Most BBHs thus far observed by LIGO-Virgo-KAGRA (the LVK) are inspiral-dominated. However, for high-mass systems, the inspiral is difficult to observe with ground-based interferometers because the majority of GWs emitted before the merger are at a lower frequency than their sensitivity band [1]. Because the inspiral period is difficult to probe directly for these systems, it is useful to be able to infer the properties of the inspiral period based on the frequencies observed in the more readily visible ringdown. The ringdown is the period directly after the merger in which the two BHs have now coalesced into a single remnant BH, and the remnant rotates asymmetrically about its axis. This perturbed BH remnant still emits GWs as it equilibrates to its final stage, a Kerr BH [2].

The ringdown GW signal consists of a sum of damped oscillations known as quasinormal modes (QNMs) [3–7], which are emitted from the perturbed BH at fundamental and overtone frequencies. They are called "quasi" because they decay over time, whereas normal modes do not. The longest lasting of these are referred to as the fundamentals, while any shorter lived modes are the overtones. The observed ringdown signal from a BBH merger is a sum of all the QNMs with some relative amplitudes and phases. In this project, we measure QNMs from simulated GW signals to see if our predictions are consistent with the true parameters in the simulation.

We simulate full inspiral-merger-ringdown signals using numerical relativity (NR) surrogate waveform models [8]. By looking at the NR surrogate model, we can see the whole waveform while knowing the mass ratio and spins of the progenitor BHs. Then, using the QNM model, we can dissect the ringdown portion of the waveform into its individual QNM components. If the QNM model predicts parameters that are consistent with the NR surrogate, this method will then be applied to real GW data to estimate inspiral parameters that cannot be observed directly.

Presently, inferring inspiral parameters (i.e., component masses and spins) from ringdown analysis is best understood when the progenitor BHs have spins aligned with the binary's orbital angular momentum. For the aligned-spin case, the relationships between QNM amplitudes and phases and the masses/spins of the inspiraling black holes have been encoded in fitting formulas or surrogate models by various authors [9–12]. Amplitudes of different modes respond differently to changing mass ratio, c.f., Fig. 4. However, in reality, most BHs possess at least some degree of spin-orbit misalignment [13], leading to spin-orbit precession. Since applying aligned-spin models to systems with precession may bias the recovery of system parameters, it is important to understand how precession affects the ringdown. Currently, the mapping from QNM amplitudes to inspiral properties is less clear for precessing binaries, although a relationship is expected [2]. The precessing case is particularly of interest because of its potential to give insight into how a BBH system formed, e.g., [14, 15]. By studying if and how the properties of the individual progenitor BHs in precessing systems can be predicted and inferred using just their ringdown data, the population of BHs that un-

dergo a merger can be better examined.

The need to understand the relationship between the inspiral and ringdown properties for high-mass (e.g. ringdown-dominated) precessing systems is further motivated by the fact that several of the BBHs observed by LIGO are indeed high-mass systems with intriguing spins. GW190521 is the second most-massive BBH system observed by LIGO and is highly precessing [16]. Its precession measurement stems from the subtle interplay between the quiet final inspiral cycle and the loud merger [17]. GW191109 and GW200129 are other high-mass systems with interesting spin configurations, but are plagued by data-quality issues: the anti-algined spin of GW191109 spins [18] and the precession in GW200129 [19] are both degenerate with glitches which are coincident with their inspirals. Finally, the new event GW231123 [20] is the most massive BBH detected yet by a factor of $\sim$ 2, and its inferred spin configuration is highly dependent on the specific waveform model used. For all of these events, the information about spins is coming primarily from their inspiral, which is either short/quiet and/or affected by data quality issues or waveform systematics, so having ways to infer the inspiral properties *without* looking at this finicky inspiral itself serves as motivation for our study.

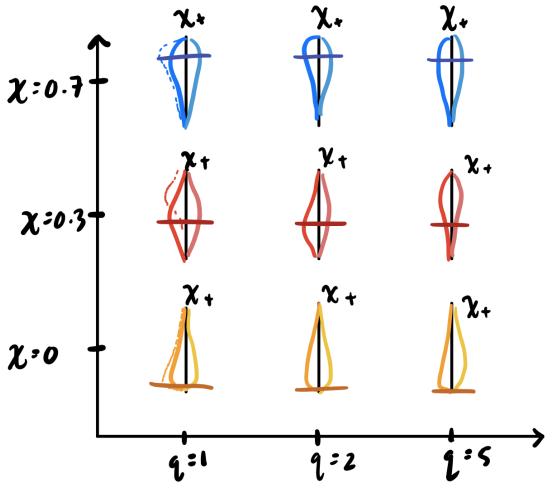

FIG. 1: Sketch of a violin plot showing posterior distributions on the inspiral spin parameter χ_+ (also known as $\chi_{\rm eff}$) [12]. In this sketch, the lighter color represents the *reconstructed* χ_+ parameter using the QNM fits; the darker color is χ_+ *directly inferred* with the NR surrogate when the full (dashed) or just ringdown (solid) data are analyzed. Each violin is from a simulated signal with a different primary spin $\chi_1 = \chi$ (vertical axis) and mass ratio q (horizontal axis). In practice, a version of this plot would be generated for each inspiral parameter we are measuring, for both the aligned and precessing cases.

II. OBJECTIVES

The purpose of this project is to test how well QNM models in the ringdown can be used to back-infer properties of the inspiral. We will start with the aligned-spin case, where the mapping from QNM amplitudes to inspiral properties is comparatively well understood [9–12], and then move on to the precessing case. We begin by analyzing simulated signals (for which we know the inspiral properties exactly); from these we can test the validity of our mappings between QNMs and inspiral properties before moving on to apply the method to real GW data. Our objectives are as follows:

1. Generate mapping between QNMs and inspiral properties (mass ratio and spins). Use this mapping to get point-estimate fits for inspiral properties of a simulated signal given only that signal's ringdown.

2. Examine how the accuracy of the fits changes for different simulated signals, e.g., equal vs. unequal masses, large vs. small spins aligned vs. precessing spins. Determine how many and which QNMs are needed to make the most accurate least-squares fit for the different simulated signals.

3. Repeat the above analyses, but instead of using point estimates, perform full parameter estimation and obtain posterior distributions on QNMs and inspiral properties, to determine if the QNM model and NR surrogate simulations agree on inspiral spin parameters for the aligned and precessing spin cases. Figure 1 shows a sketch of what these posteriors might look like.

4. Apply our method to a real GW signal, like GW231123 or GW190521.

While we aspire to investigate the full spin degrees of freedom, mappings for the QNM amplitudes in the precessing case are not well understood, although see Refs. [2, 21] for work in this direction. Consequently, a simpler question we could ask is when do the aligned-spin mappings break down (say, as a function of SNR and how much precession there is).

III. METHODS

So far in this project, we have been working on developing a method for mapping between QNMs and inspiral properties (see Point 1 in Sec.II). The method consists of utilizing NR surrogate waveforms and QNM models to compare ringdown signals and determine if the QNM model can accurately infer the inspiral parameters. Section III A outlines the process for testing surrogates for the aligned spin case. After finding surrogates that agree well with the QNM model, these surrogates can be in-

verted to return inspiral parameters. This process is discussed in Sec. III B.

The following is an overview of our method. The NR surrogate NRHybSur3dq8 [22] will yield a complete inspiral-merger-ringdown (IMR) waveform. Then `qnmfits` will be implemented to make a fit for just the ringdown of the NRHybSur3dq8 waveform. By inverting an additional *remnant* NR surrogate NRSur3dq8_RD, the amplitude and phase observed in the ringdown can be mapped back to inspiral parameters.

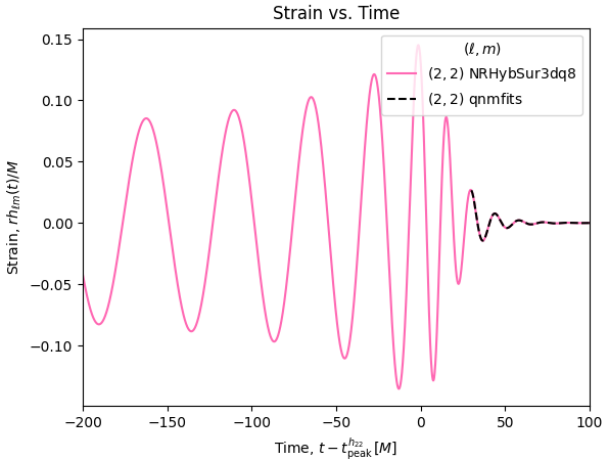

FIG. 2: Plot of full waveform from NRHybSur3dq8 and model from `qnmfits` for $t_0 = 30M$

Closer to the time of the merger, nonlinearities cause the QNM model to break down [23]. To make the QNM model valid, we must start at some time after the merger, which is defined as the peak strain of the quadrupole mode. The quadrupole mode is expected to be dominant in systems with equal masses and aligned spins, but higher harmonics are expected to be much more important in precessing systems [24]. In Fig. 2, the start time is $t_0 = 30M$. Other surrogates define t_0 at different times. We use a least-squares fit with the Python package `qnmfits` to determine which combination of QNMs yields the observed NRHybSur3dq8 waveform. Because all QNMs must agree on the same mass and spin for a BH remnant, there are a limited number of combinations of QNMs that could produce an observed signal.

A. Testing Surrogates for Aligned Spin Systems

Figure 3 shows strain vs. time for NRHybSur3dq8 [22] with different mass ratios to demonstrate how the amplitudes of the waves vary for different modes. This initial step motivates modeling the relationship between amplitude and mass ratio directly for different modes. The final product of examining this graph was to plot the relationship between amplitude and mass ratio for different modes, c.f., Fig. 4. This relationship is useful because it

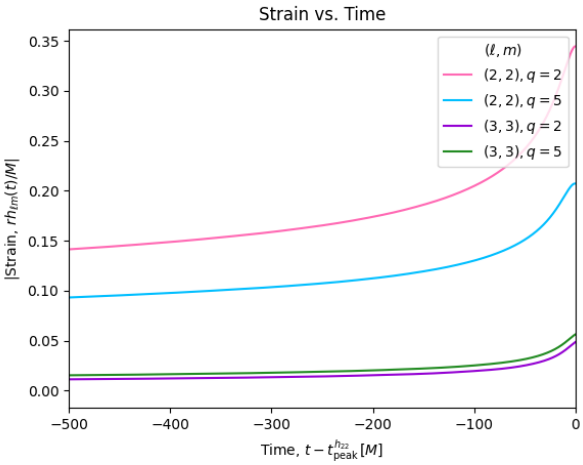

FIG. 3: Plot of strain vs. time for the (3,3) and (2,2) modes for $q = 2$ and $q = 5$.

directly relates amplitude, a property directly measurable in the ringdown, and mass ratio, a property relating the progenitor BHs.

Dimensionless strains for QNMs are related to the amplitude by:

$$\begin{aligned} h_{\ell mn} &\sim C_{\ell mn} e^{-i\omega_{\ell mn} t} \\ &\sim A_{\ell mn} e^{i\phi_{\ell mn}} e^{-i(2\pi f_{\ell mn} - i/\tau_{\ell mn})t} \end{aligned}$$

where h is dimensionless strain, C is the complex amplitude, A is the real amplitude, and τ is the damping time. The amplitudes obtained from `qnmfits`, C, are complex amplitudes, and also require a correction to account different start times in different fits,

$$C_{\rm corrected} = C e^{-i\omega \Delta t}$$

where Δt is the difference in time between the start of a fit and a reference time $t_{\rm ref}$ we are propagating back to. In this project, we propagate all fits back to $t_{\rm ref} = 0$ to compare them more easily.

Taking the absolute value of the complex amplitudes yields the real amplitudes, A. Similarly, finding the angle counterclockwise from the positive real axis in the complex plane gives the phase, ϕ. These quantities will be useful when a remnant surrogate is eventually inverted to take amplitude and phase as inputs and return mass ratio and spins.

The results of plotting corrected amplitudes from `qnmfits` against mass ratio were compared to functions from `jaxqualin` code [25], c.f., Fig. 5a. `Jaxqualin` code provides functions of mass ratio for both the amplitude and phase. Although the `qnmfits` and `jaxqualin` amplitude models agreed reasonably well, the phases were substantially discrepant, as can be seen in Fig. 5b. A new surrogate, NRSur3dq8_RD was implemented to see if it aligned with NRHybSur3dq8 more closely. It matched

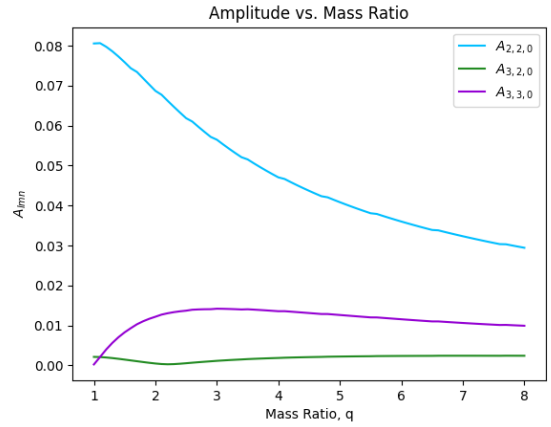

FIG. 4: Plot of corrected amplitude vs. mass ratio for selected modes from NRHybSur3dq8.

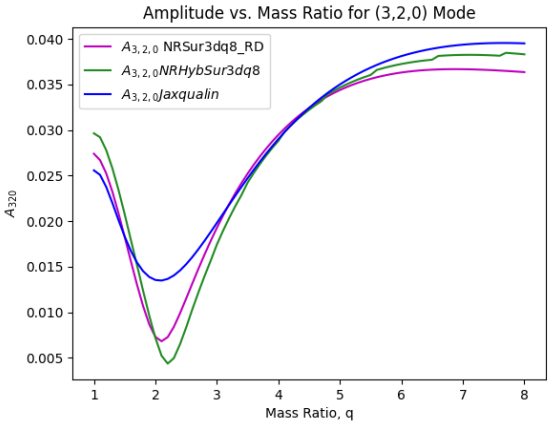

(a) Plot of amplitude vs mass ratio for NRSur3dq8_RD, NRHybSur3dq8, and `jaxqualin`.

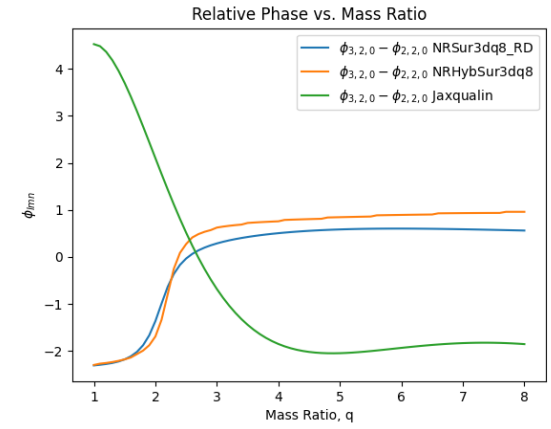

(b) Plot of relative phase for (3,2,0) mode vs mass ratio forNRSur3dq8_RD, NRHybSur3dq8, and `jaxqualin`.

FIG. 5: These plots compare amplitude and relative phase plotted against mass ratio for selected modes in NRSur3dq8_RD, NRHybSur3dq8, and `jaxqualin`.

NRHybSur3dq8 more closely in amplitude and relative phase than the `jaxqualin` fit.

Moving forward, NRSur3dq8_RD has shown to be a more effective surrogate to compare with `qnmfits` for NRHybSur3dq8. `Jaxqualin` will not be used due to the large discrepancy in phases with `qnmfits`.

B. Inverting a Surrogate

The purpose of using a surrogate that requires inspiral parameters as inputs and generates a waveform is to invert the surrogate to return inspiral parameters as outputs when given a waveform from a QNM model.

We did this by using residuals of the real and imaginary parts of the complex amplitudes from `qnmfits` for NRHybSur3dq8 to those produced by the remnant surrogate NRSur3dq8_RD to do a least squares fit and determine where the residual is minimized. This is where the remnant surrogate model and the QNM model have the smallest difference.

Shown in Fig. 6, the true values of the full IMR waveform were not perfectly predicted by the remnant surrogate. These plots are all for the aligned spin case where each BH spin only has a z component. This motivates investigating other remnant surrogate models to determine how much these discrepancies are surrogate dependent or if they are a result of varying true system parameters.

IV. FUTURE WORK

A current problem is that the remnant surrogate NRSur3dq8_RD does not seem to predict the true parameters as accurately in cases with more extreme mass ratios and spins. This motivates investigating if accuracy of the fit varies between as different QNMs are included/excluded, and if so, which QNMs are necessary to most accurately recover parameters. Similarly, it is worth exploring the limits of q, χ_1, and χ_2 and what values cause inferred parameters to be less accurate. A useful approach to solving this will be to test other remnant surrogates and determine which model can most accurately predict the true parameters. This addresses Point 2 in Sec. II.

So far, we have only generated point estimates for different combinations of QNMs that could yield an observed waveform. Moving forward, we will generate a posterior distribution and do full parameter estimation, addressing Point 3 in Sec. II.

The ultimate goal is to produce a similar model to map between QNMs and inspiral parameters for the precessing case. However, modeling the precessing case is much more difficult. A useful intermediate step would be to determine at what spin limits aligned spin analysis breaks down. If we can produce an effective model for precessing systems, the result could be applied to real GW data, such as GW231123 or GW190521 (Point 4 in Sec. II).

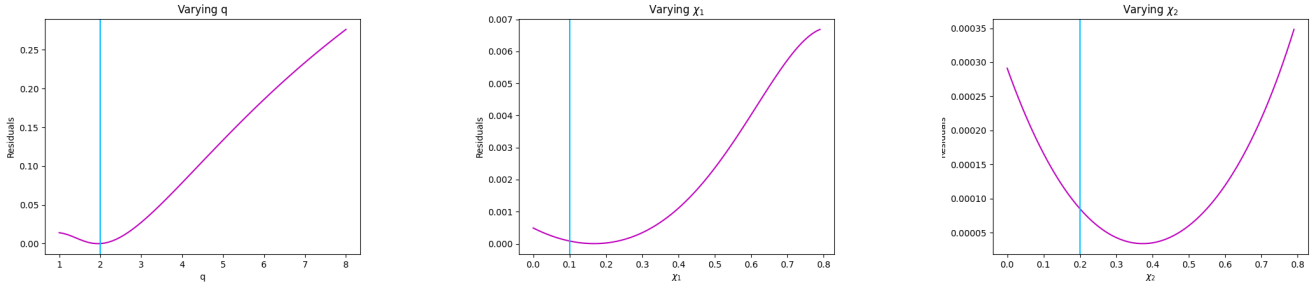

(a) Varying q while $\chi_1 = 0.1$ and $\chi_2 = 0.2$

(b) Varying χ_1 while $q = 2$ and $\chi_2 = 0.2$

(c) Varying χ_2 while $q = 2$ and $\chi_1 = 0.1$

FIG. 6: These plots show the residuals of the complex amplitudes (magenta) from the NR surrogate model and the QNM model plotted against q, χ_1, and χ_2 where one of these parameters varies on the x-axis and the other two are held constant. The true values for q, χ_1, and χ_2 are shown by the vertical turquoise lines.

[1] A. Buikema *et al.*, Phys. Rev. D **102**, 062003 (2020), arXiv:2008.01301 [astro-ph.IM].
[2] H. Zhu *et al.*, Phys. Rev. D **111**, 064052 (2025), arXiv:2312.08588 [gr-qc].
[3] S. A. Teukolsky, Astrophys. J. **185**, 635 (1973).
[4] S. Chandrasekhar and S. Detweiler, Proceedings of the Royal Society of London Series A **344**, 441 (1975).
[5] K. D. Kokkotas and B. G. Schmidt, Living Rev. Rel. **2**, 2 (1999), arXiv:gr-qc/9909058.
[6] S. Detweiler, Astrophys. J. **239**, 292 (1980).
[7] O. Dreyer, B. J. Kelly, B. Krishnan, L. S. Finn, D. Garrison, and R. Lopez-Aleman, Class. Quant. Grav. **21**, 787 (2004), arXiv:gr-qc/0309007.
[8] V. Varma, S. E. Field, M. A. Scheel, J. Blackman, D. Gerosa, L. C. Stein, L. E. Kidder, and H. P. Pfeiffer, Phys. Rev. Research. **1**, 033015 (2019), arXiv:1905.09300 [gr-qc].
[9] L. London, D. Shoemaker, and J. Healy, Phys. Rev. D **90**, 124032 (2014), [Erratum: Phys.Rev.D 94, 069902 (2016)], arXiv:1404.3197 [gr-qc].
[10] L. T. London, Phys. Rev. D **102**, 084052 (2020), arXiv:1801.08208 [gr-qc].
[11] S. Borhanian, K. G. Arun, H. P. Pfeiffer, and B. S. Sathyaprakash, Class. Quant. Grav. **37**, 065006 (2020), arXiv:1901.08516 [gr-qc].
[12] M. H.-Y. Cheung, E. Berti, V. Baibhav, and R. Cotesta, Phys. Rev. D **109**, 044069 (2024), [Erratum: Phys.Rev.D 110, 049902 (2024)], arXiv:2310.04489 [gr-qc].
[13] R. Abbott *et al.* (KAGRA, VIRGO, LIGO Scientific), Phys. Rev. X **13**, 041039 (2023), arXiv:2111.03606 [gr-qc].
[14] C. L. Rodriguez, M. Zevin, C. Pankow, V. Kalogera, and F. A. Rasio, Astrophys. J. Lett. **832**, L2 (2016), arXiv:1609.05916 [astro-ph.HE].
[15] I. Mandel and A. Farmer, Phys. Rept. **955**, 1 (2022), arXiv:1806.05820 [astro-ph.HE].
[16] R. Abbott *et al.*, Physical Review Letters **125** (2020), 10.1103/physrevlett.125.101102.
[17] S. J. Miller, M. Isi, K. Chatziioannou, V. Varma, and I. Mandel, Physical Review D **109** (2024), 10.1103/physrevd.109.024024.
[18] R. Udall, S. Hourihane, S. Miller, D. Davis, K. Chatziioannou, M. Isi, and H. Deshong, Physical Review D **111** (2025), 10.1103/physrevd.111.024046.
[19] E. Payne, S. Hourihane, J. Golomb, R. Udall, D. Davis, and K. Chatziioannou, Physical Review D **106** (2022), 10.1103/physrevd.106.104017.
[20] A. G. Abac *et al.* (LIGO Scientific, Virgo, KAGRA), "GW231123: gravitational-wave observation of a binary black hole merger with a total mass of about 240 ," (2025), citation to be filled by journal.
[21] F. Nobili, S. Bhagwat, C. Pacilio, and D. Gerosa, (2025), arXiv:2504.17021 [gr-qc].
[22] V. Varma, S. E. Field, M. A. Scheel, J. Blackman, L. E. Kidder, and H. P. Pfeiffer, Physical Review D **99** (2019), 10.1103/physrevd.99.064045.
[23] E. Finch, *Black-hole Ringdown*, Ph.D. thesis, University of Birmingham (2023).
[24] J. Roulet and T. Venumadhav, Annual Review of Nuclear and Particle Science **74**, 207–332 (2024).
[25] M. H.-Y. Cheung, E. Berti, V. Baibhav, and R. Cotesta, Physical Review D **109** (2024), 10.1103/physrevd.109.044069.